

**FEDSM-ICNMM2010-3\$) \$-**

## **YIELD STRESS FLUID METHOD TO MEASURE THE PORE SIZE DISTRIBUTION OF A POROUS MEDIUM**

**Oukhleif Aimad**

Arts et Métiers ParisTech/EMT  
2 bd du Ronceray, BP 93525, 49035 Angers  
cedex 1, France

**Champmartin Stéphane**

Arts et Métiers ParisTech/EMT  
2 bd du Ronceray, BP 93525, 49035 Angers  
cedex 1, France

**Ambari Abdlehak**

Arts et Métiers ParisTech/EMT  
2 bd du Ronceray, BP 93525, 49035 Angers  
cedex 1, France

**Despeyroux Antoine**

Arts et Métiers ParisTech/EMT  
2 bd du Ronceray, BP 93525, 49035 Angers  
cedex 1, France

### **ABSTRACT**

In this paper a new method is presented in order to determine the pore size distribution in a porous media. This original technique uses the non Newtonian yield-pseudo-plastic rheological properties of some fluid flowing through the porous sample. In a first approximation, the very well-known and simple Carman-Kozeny model for porous media is considered. However, despite the use of such a huge simplification, the analysis of the geometry still remains an interesting problem. Then, the pore size distribution can be obtained from the measurement of the total flow rate as a function of the imposed pressure gradient. Using some yield-pseudo-plastic fluid, the mathematical processing of experimental data should give an insight of the pore-size distribution of the studied porous material. The present technique was successfully tested analytically and numerically for classical pore size distributions such as the Gaussian and the bimodal distributions using Bingham or Casson fluids (the technique was also successfully extended to Herschel-Bulkley fluids but the results are not presented in this paper). The simplicity and the cheapness of this method are also its assets.

### **INTRODUCTION**

Porous media are found literally everywhere around us [1-3], in Nature (soils, human skin, sedimentary rocks...) as well as in engineering and applied scientific domains (groundwater, petroleum engineering, filtration, powder, concrete, cement...). Except maybe the metals, some very dense minerals and the plastic materials, every piece of matter is porous if it is studied

at a sufficiently small geometrical scale. Since the early work of Darcy [4], the transport phenomena and the flows through porous media generated an important research activity which is still relevant today. The technological applications involving porous media are very numerous and will keep on growing in the future because of the increase of the energy cost and the realization of environmental challenges. For example let us cite the recent application for solar collectors of heat storage in granular porous media. Another instance concerns the heat storage for human housing using porous phase change materials. The continuous decrease of conventional oil and gas reserves implies a high level of investments for tertiary recovery techniques in particular for bituminous sands and oil shale which are also saturated porous media. The storage and the behavior of pollutants in porous matter (hazardous wastes, CO<sub>2</sub> sequestration...) are topics for which it is essential to have a deep knowledge and an accurate characterization of porous media.

The strong dependence of the transport properties (permeability, diffusivity) in porous media with the size of their pores constitutes a challenge in many scientific areas. Many techniques were developed in order to measure the pore size distribution (PSD<sup>1</sup>). Let us cite for example the mercury intrusion porosimetry (MIP<sup>2</sup>) [1-3,5] consisting in the injection of mercury in the porous medium. As most materials are not wetted by mercury, a pressure gradient must be imposed to induce a flow. For a given injection pressure P, mercury can

---

<sup>1</sup> Pore Size Distribution

<sup>2</sup> Mercury Intrusion Porosimetry

only invade the pores which radius are greater than  $2\sigma_{lg} \cos \theta / P$  where  $\sigma_{lg}$  and  $\theta$  are respectively the liquid/gas interfacial tension and the contact angle. The pore size volume distribution is obtained with the derivative of the curve representing the volume of the invaded pores according to the radius of the pores. Because of the toxicity of mercury, this technique is intended to phase out. Another technique based on the calorimetric analysis (DSC<sup>3</sup>) of the liquid-solid phase transition of the fluid in a porous media is called thermoporosimetry [6-8]. This alternative method for determining the PSD in porous materials, suggested by Kuhn and later derived by Brun et al. [9], uses a thermodynamical relationship between the depression in the triple point temperature of the confined liquid and the radius of the pore where the phase transition occurs. It is expressed by the Gibbs-Thomson equation:  $\Delta T / T_0 = 2\sigma_{ls} v_l / \Delta H_0 R_p$ , where  $\sigma_{ls}$  is the liquid/solid interfacial tension,  $v_l$  the liquid phase molar volume,  $\Delta H_0$  the molar heat of fusion,  $R_p$  the pore radius, and  $T_0$  being the triple point temperature of the liquid. The principle of the method is based on the lowering of the triple point temperature of a liquid filling a porous material. The phase transitions (crystallization or melting) for a liquid confined within a pore are observed to shift to lower temperatures that are determined by the pore size. This difference in transition temperature  $\Delta T$ , between confined and bulk liquid can be detected calorimetrically by DSC. A thermodynamic method makes it possible to measure the specific surface of a solid by model BET of a multi-layer adsorption [10]. The pore radius distribution can also be extracted using for example the DFT<sup>4</sup> method [11] based on statistical mechanics, which connects macroscopic properties to the molecular behavior and B.J.H. method [12]. This classical method uses the isothermal desorption due to the molecular Van der Waals interactions between a condensing vapor and the internal surface of the pores. Finally let us quote destructive techniques such as stereology [13] or non destructive methods such as Small Angle Neutron or X-Ray Scattering (SANS<sup>5</sup> or SAXS<sup>6</sup>) [14,15], NMR<sup>7</sup> [16] etc. Unfortunately the various cited experimental approaches can give quite different results and are very expensive. Therefore an alternative simpler and cheaper technique is proposed in order to characterize the PSD of a porous medium. The next paragraph presents and develops this new method.

## PRESENTATION OF THE MODEL

This model presented here is based on the existence of the threshold in the rheological behavior of some non Newtonian pseudo-plastic fluid such as Bingham, Casson or Herschel-Bulkley fluids. The basic idea is the following: in order to set

such fluids into motion, it is necessary to impose between both ends of a pore a pressure gradient ( $\nabla P$ ) greater than a critical value depending, for a given fluid yield stress ( $\tau_0$ ), on the pore radius ( $r$ ). As the pressure gradient grows, more and more fluid flows through the porous sample via the pores which have the radius greater than the critical one corresponding to the pressure gradient imposed. The flow of a Bingham fluid is analyzed in the first place.

### Bingham model

Such fluids obey the following rheological behavior law:

$$\begin{cases} \underline{\underline{\tau}} = 2 \left( \mu - \frac{\tau_0}{\sqrt{2\underline{\underline{D}} : \underline{\underline{D}}}} \right) \underline{\underline{D}} & \text{for } \sqrt{\frac{\underline{\underline{\tau}} : \underline{\underline{\tau}}}{2}} \geq \tau_0 \\ \underline{\underline{D}} = 0 & \text{for } \sqrt{\frac{\underline{\underline{\tau}} : \underline{\underline{\tau}}}{2}} < \tau_0 \end{cases} \quad (1)$$

with  $\underline{\underline{\tau}}$  the viscous stress tensor,  $\underline{\underline{D}}$  the rate of deformation tensor and  $\mu$  the constant plastic viscosity of the fluid. The well-known Kozeny-Carman capillary model for the porous medium is adopted: it is composed of  $N$  parallel capillaries (Fig. 1); the pore radii of which are distributed according to the probability density function  $p(r)$ . When a pressure gradient  $\nabla P$  is imposed at both ends of this system, the fluid flows through it at the flow rate  $Q(\nabla P)$ . This total flux is related to the elementary flow rate  $q(\nabla P, r)$  in a capillary of radius  $r$  and to  $p(r)$  by a Volterra integral equation of the first kind:

$$Q(\nabla P) = \int_{r_0 = \frac{2\tau_0}{\nabla P}}^{\infty} q(\nabla P, r) p(r) dr \quad (2)$$

the kernel of which is:

$$\begin{cases} q(\nabla P, r) = \frac{\pi \tau_0 r^4}{4\mu r_0} \left( 1 - \frac{4}{3} \left( \frac{r_0}{r} \right) + \frac{1}{3} \left( \frac{r_0}{r} \right)^4 \right) & \text{for } r \geq r_0 \text{ and } \tau_0 = \frac{\nabla P r_0}{2} \\ q(\nabla P, r) = 0 & \text{for } r < r_0 \end{cases} \quad (3)$$

As long as  $r < r_0$  the fluid does not flow.  $r_0$  is also the radius of the core zone of the Bingham plug flow.

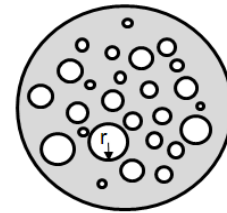


Figure 1: Kozeny-Carman model

<sup>3</sup> Differential Scanning Calorimetry

<sup>4</sup> Density Functional Theory

<sup>5</sup> Small Angle Neutron Scattering

<sup>6</sup> Small Angle X-Ray Scattering

<sup>7</sup> Nuclear Magnetic Resonance

The pore size distribution  $p(r)$  can be obtained through a differential operator applied to  $Q(\nabla P)$  [17]:

$$p(r) = \frac{\mu(\nabla P)^2}{\pi\tau_0 r^4} \left[ 5 \frac{\partial^2 Q}{\partial \nabla P^2} + \nabla P \frac{\partial^3 Q}{\partial \nabla P^3} \right]_{\left( \nabla P = \frac{2\tau_0}{r} \right)} \quad (4)$$

To verify the applicability of this formula, let us assume that the PSD can be described by a Gaussian distribution of mean value  $m$  and standard deviation  $\sigma$ . If  $m$  is taken as characteristic length scale and  $2\tau_0/m$  as characteristic pressure gradient scale, it is possible to normalize the Volterra integral equation (2) as follows:

$$Q^+(\nabla P^+) = \int_{r_0^+ = \frac{1}{\nabla P^+}}^{\infty} q^+(\nabla P^+, r^+) p^+(r^+) dr^+ \quad (5)$$

The Fig. 2 below shows the normalized total flow rate versus the normalized pressure gradient resulting from the flow of the Bingham fluid through a porous medium with a given Gaussian distribution PSD.

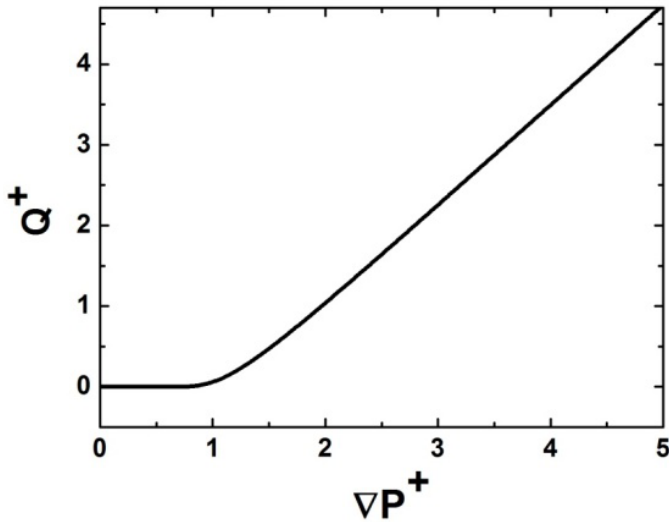


**Figure 2: Total flow rate vs. pressure gradient for a Gaussian distribution and a Bingham fluid**

This figure is characterized by a first region at low pressure gradients in which the flow rate is zero. This region extends up to  $\nabla P^+ = 1$ . It is followed by a second region in which the flow rate varies linearly with the pressure gradient, due to the fact that the plastic viscosity is constant, beyond the pressure gradient threshold. The non-dimensional elementary flow in a single capillary tube is:

$$\begin{cases} q^+(\nabla P^+, r^+) = He \left( \nabla P^+ r^{+4} - \frac{4}{3} r^{+3} + \frac{1}{3} \frac{1}{\nabla P^{+3}} \right) & \text{for } r^+ \geq r_0^+ \\ q^+(\nabla P^+, r^+) = 0 & \text{for } r^+ < r_0^+ \end{cases} \quad (6)$$

with the Hedström number  $He = \rho\tau_0(2m)^2 / \mu^2$ . The PSD can now be written as follows:

$$p^+(r^+) = \frac{(\nabla P^+)^6}{4He} \left( 5 \frac{\partial^2 Q^+}{\partial \nabla P^{+2}} + \nabla P^+ \frac{\partial^3 Q^+}{\partial \nabla P^{+3}} \right)_{\nabla P^+ = \frac{1}{r^+}} \quad (7)$$

Equation 7 is called the “Pore Size Distribution Equation” or PSDE.

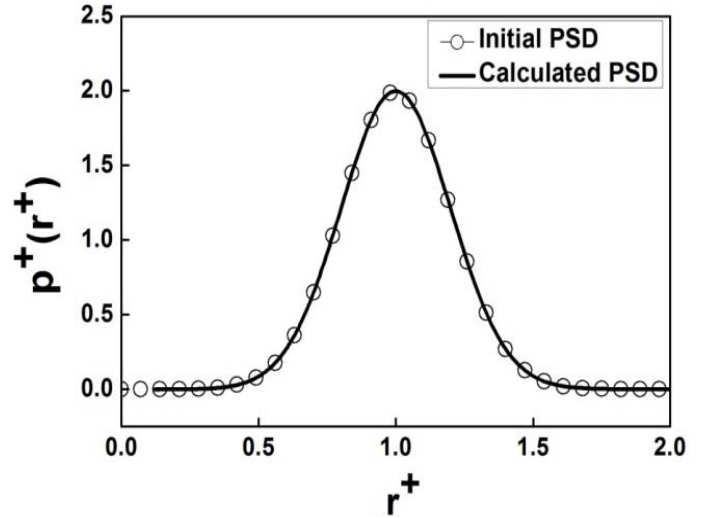


**Figure 3: Comparison between the initial and the calculated PSD**

In a second step, the given distribution is ignored and the flow rate-pressure gradient curve given by the initial calculation (or given by an experiment) is used as a starting point. Then Eq. 7 is applied to the flow rate-pressure gradient characteristic, and the following Fig. 3 which is obtained in the case  $He = 1$ . This figure exhibits a perfect agreement between the original Gaussian distribution and the distribution calculated with the relationship obtained for  $p^+(r^+)$ . To verify the efficiency of this technique with more complex distributions, a bimodal distribution is considered, with two peaks at  $m_1$  and  $m_2 = 2m_1$  and the same standard deviation  $\sigma$  (for instance) such as:

$$p^+(r^+) = \frac{1}{2} \left( \frac{m_1}{\sigma\sqrt{2\pi}} \exp \left[ \frac{-(r^+ - 1)^2}{2\sigma^2/m_1^2} \right] + \frac{m_1}{\sigma\sqrt{2\pi}} \exp \left[ \frac{-(r^+ - (m_2/m_1))^2}{2\sigma^2/m_1^2} \right] \right) \quad (8)$$

in which the radius and the PSD are scaled with  $m_1$ . The total flow rate  $Q^+$  is obtained in this case; the result is shown in Fig. 4.

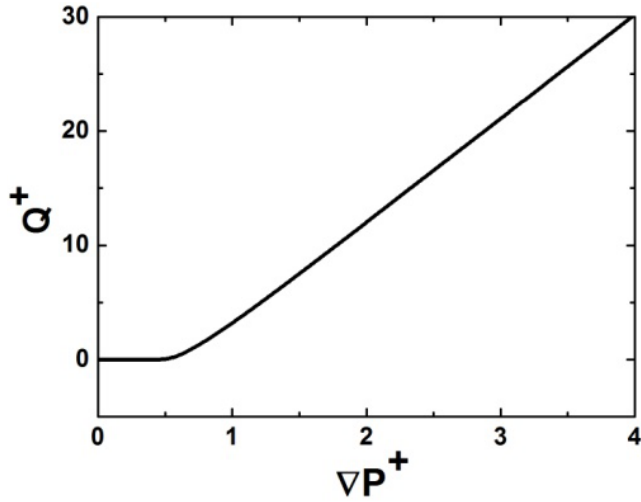


**Figure 4: Total flow rate vs. pressure gradient for a bimodal distribution with  $m_2 = 2m_1$  and a Bingham fluid**

This figure brings out that the threshold between both regions discussed earlier is derived for  $\nabla P^+ = 0.5$  because  $m_2 = 2m_1$  in our example. Now if Eq. 7 is applied to the characteristic shown in Fig. 4, the result is plotted in Fig. 5 below. Once again one can notice the good agreement between the initial PSD and the calculated PSD ( $He = 1$ ).

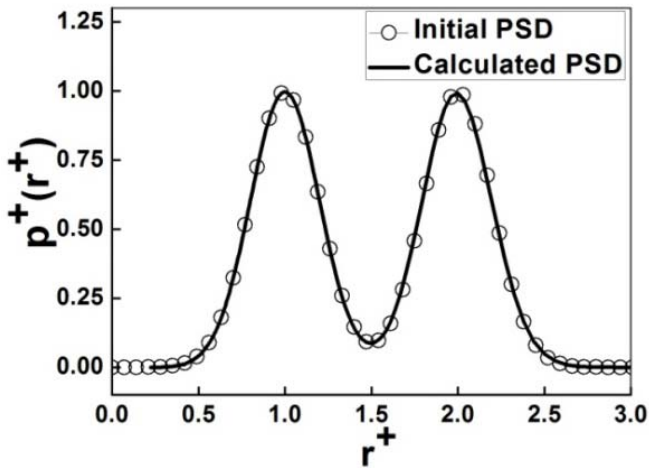


**Figure 5: Comparison between the initial and the calculated PSD for a bimodal distribution with  $m_2 = 2m_1$  and a Bingham fluid**

In the next paragraph the case of a more complex pseudo-plastic fluid will be discussed: the Casson fluid.

#### Casson model

In this model the rheological behavior law of the fluid is:

$$\begin{cases} \tau_{rz}^{1/2} = \tau_0^{1/2} + \mu^{1/2} \left( -\frac{\partial u_z}{\partial r} \right)^{1/2} & \text{for } \tau_{rz} \geq \tau_0 \\ \frac{\partial u_z}{\partial r} = 0 & \text{for } \tau_{rz} < \tau_0 \end{cases} \quad (9)$$

The elementary flow rate in a circular capillary tube can be written as in [18]:

$$\begin{cases} q(\nabla P, r) = \frac{\pi \tau_0 r^4}{4\mu r_0} \left( 1 - \frac{16}{7} \left( \frac{r_0}{r} \right)^{1/2} + \frac{4}{3} \left( \frac{r_0}{r} \right) - \frac{1}{21} \left( \frac{r_0}{r} \right)^4 \right) \\ \text{for } r \geq r_0 \text{ where } \tau_0 = \frac{\nabla P r_0}{2}; \text{ and } q(\nabla P, r) = 0 \text{ for } r < r_0 \end{cases} \quad (10)$$

Similarly to the previous section, the total flow rate through an array of parallel capillary tubes, the radii of which are distributed according to a PSD  $p(r)$ , is obtained with the same Volterra integral equation (Eq. 2). The determination of the probability density function  $p(r)$  of this integral equation leads to the new PSDE:

$$p^+(r^+) = \frac{(\nabla P^+)^6}{2He} \left( \frac{15}{2} \frac{\partial^2 Q^+}{\partial \nabla P^{+2}} + \frac{15}{2} \nabla P^+ \frac{\partial^3 Q^+}{\partial \nabla P^{+3}} + (\nabla P^+)^2 \frac{\partial^4 Q^+}{\partial \nabla P^{+4}} \right)_{\nabla P^+ = \frac{1}{r^+}} \quad (11)$$

where the radius and the PSD are normalized by the characteristic mean length scale  $m$  and the pressure gradient by the characteristic pressure gradient scale  $2\tau_0/m$ . If the PSD is supposed to be of the Gaussian type, the total flow rate thus obtained is presented in Fig. 6.

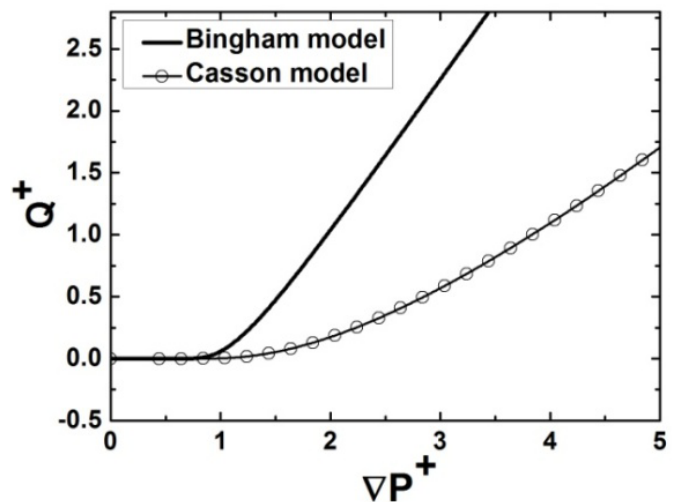


**Figure 6: Total flow rate vs. pressure gradient for a Gaussian distribution (Casson and Bingham fluids)**

This figure also presents for comparison the characteristic curve for a Bingham fluid. The total flow rate for a Casson fluid exhibits a less steep evolution than the flow rate for a Bingham fluid.

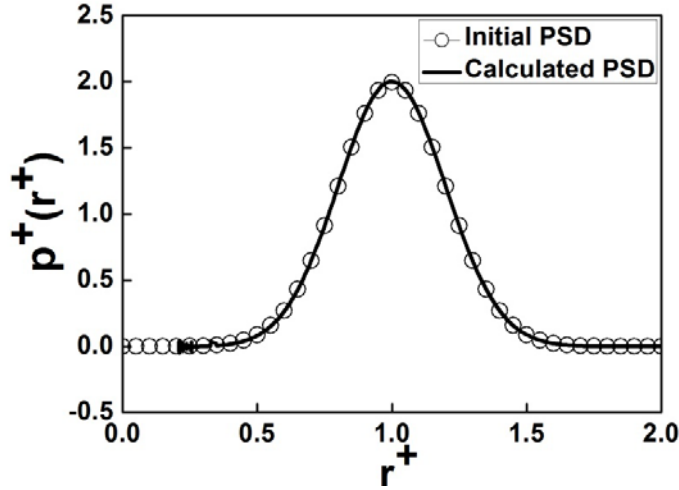


Figure 7: Comparison between the initial and the calculated PSD for a Gaussian distribution and a Casson fluid

Once again when Eq. 11 is applied to the results given in the Casson curve plotted in Fig. 6, the initially injected Gaussian PSD is retrieved (see Fig. 7 above). Finally for a bimodal distribution with  $m_2 = 2m_1$  and  $\sigma_2 = 5\sigma_1/2$ , the characteristic curve in Fig. 8 is obtained and one more time the application of the new PSDE (Eq. 11) recovers the initial density probability function as shown in Fig. 9.

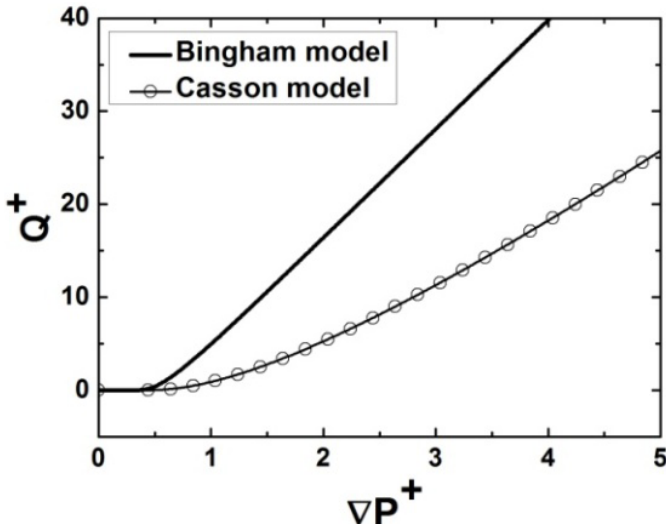


Figure 8: Total flow rate vs. pressure gradient for a bimodal distribution with  $m_2 = 2m_1$  and  $\sigma_2 = 5\sigma_1/2$  (Casson and Bingham fluids)

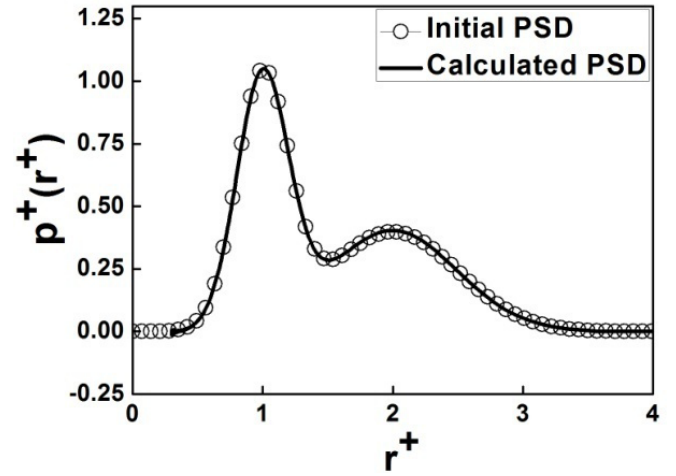


Figure 9: Comparison between the initial and the calculated PSD for a bimodal distribution with  $m_2 = 2m_1$  and  $\sigma_2 = 5\sigma_1/2$  for a Casson fluid

This method is therefore as effective and robust for a Casson fluid as for a Bingham fluid regardless the initial distribution. This technique was also tested for Herschel-Bulkley fluids with the same success.

## CONCLUSION

In this paper we presented an original method giving the pore size distribution in a porous medium provided that the Kozeny-Carman model can be used. This method is based on the existence of a yield stress in non Newtonian pseudo-plastic fluids. This threshold leads to a Volterra integral equation of the first kind. The mathematical determination of the probability density function  $p(r)$  in this integral is possible using the partial fractional or non fractional derivatives of the total flow rate of fluid through the porous medium as a function of the pressure gradient. This technique was successfully tested for Bingham and Casson fluids in the case of classical Gaussian and bimodal distribution. Nevertheless any other distribution could be used. This method was also extended to Herschel-Bulkley fluid with the same achievement.

## NOMENCLATURE

$\underline{\underline{D}}$  : rate of deformation tensor  $[s^{-1}]$

$He = \rho\tau_0(2m)^2 / \mu^2$  : Hedström number

$\Delta H_0$  : molar heat of fusion  $[J.mol^{-1}]$

$m, m_1, m_2$  : characteristic mean length scales of the Gaussian and the bimodal distributions  $[m]$

$\nabla P$  : pressure gradient  $[Pa.m^{-1}]$

$\nabla P^+ = m\nabla P / 2\tau_0$  : non-dimensional pressure gradient

$p(r)$  : probability density function of the pore size  $[m^{-1}]$

$p^+(r^+) = m.p(r)$ : non-dimensional pore size distribution  
 $q_c = \pi \mu m / 16 \rho$ : characteristic flow rate for Bingham and Casson fluids  $[m^3.s^{-1}]$   
 $Q$ : total flows rate through a porous medium  $[m^3.s^{-1}]$   
 $Q^* = Q/q_c$ : non-dimensional total flow rate through a porous medium  
 $q$ : elementary flow rate in a capillary of radius  $r$   $[m^3.s^{-1}]$   
 $q^+ = q/q_c$ : non-dimensional flow rate in a capillary  
 $r$ : pore radius  $[m]$   
 $r^+ = r/m$ : non-dimensional pore radius  
 $r_0 = 2\tau_0/\nabla P$ : critical pore radius  $[m]$   
 $r_0^+ = 1/\nabla P^+$ : non-dimensional critical pore radius  
 $\Delta T = T - T_0$ : triple point depression  $[K]$   
 $T_0$ : being the triple point temperature of the liquid  $[K]$   
 $v_l$ : liquid phase molar volume  $[m^3.mol^{-1}]$

#### Greek symbols

$\sigma$ ,  $\sigma_1$ ,  $\sigma_2$ : standard deviation of the Gaussian and the bimodal distributions  $[m]$   
 $\tau_0$ : yield stress  $[Pa]$   
 $\mu$ : constant plastic viscosity of the fluid  $[Pa.s]$   
 $\sigma_k$ : liquid/solid interfacial tension  $[J.m^{-2}]$   
 $\sigma_{lg}$ : liquid/gas interfacial tension  $[J.m^{-2}]$   
 $\theta$ : liquid/solid contact angle  
 $\underline{\underline{\tau}}$ : viscous stress tensor  $[Pa]$

#### REFERENCES

- [1] Dullien, F. A. L., 1992, *Porous media- fluid transport and pore structure*, 2<sup>nd</sup> edition, Academic Press.
- [2] Scheidegger, A. E., 1974, *The physics of flow through porous media*, 3<sup>rd</sup> edition, University of Toronto press.
- [3] Kaviany, M., 1995, *Principles of heat transfer in porous media*, 2<sup>nd</sup> edition, Springer.
- [4] Darcy, H., 1856, *Les fontaines publiques de la ville de Dijon*.
- [5] Heinemann, Z. E., 2005, *fluid flow in porous media*, Textbook series, **1**, 1-36.
- [6] Wulff, M., 2004, "Pore size determination by thermoporometry using acetonitrile", *Thermochimica Acta* **419**, 291-294.
- [7] Yamamoto, T., Endo, A., Inagi, Y., Ohmori, T., and Nakaiwa, M., 2005, "Evaluation of thermoporometry for characterization of mesoporous materials". *J. of Colloid and Interface Science* **284**, 614–620.
- [8] Nedelec, J- M., Grolier, J- P. E., and Baba, M., 2006, "Thermoporosimetry: A powerful tool to study the cross-linking in gel networks", *J Sol-Gel Sci Techn* **40**, 191–200.
- [9] Brun, M., Lallemand, A., Quinson, J-F., and Eyraud, C., 1977, *Thermochim. Acta* **21**, 59-88.
- [10] Brunauer, S., Emmett, P., and Teller, E., 1938, "Adsorption of Gases in Multimolecular Layers", *J. of the American Chemical Society*, **60**, 309-319.
- [11] Lowell, S., Shields, J. E., Thomas, M. A., and Thommes, M., 2004, *Characterization of porous solids and powders: surface area, pore size and density*, 1<sup>st</sup> edition, Kluwer Academic Publishers.
- [12] Barrett, E. P., Joyner, L. G., and Halenda, P. P., 1951, "The determination of pore volume and area distributions in porous substances computations from Nitrogen Isotherms", *J. of the American Chemical Society*, **73**, 373-380.
- [13] Haynes, J. M., 1973, "Stereological analysis of pore structure", *J. Materials and Structures* **6**, N° 3, 175-179.
- [14] Tamon, H., and Ishizaka, H., 1998, "Saxs study on gelation process in preparation of resorcinol-formaldehyde aerogel", *J. of Colloid and Interface Science* **206**, 577-582.
- [15] Pearson, D., and Allen, A. J., 1985, "A study of ultrafine porosity in hydrated cements using small angle neutron scattering", *J. of Material Science*, **20**, 303-315.
- [16] Sagidullin, A. I., and Furo, I., 2008, "Pore size distribution measurements in small samples and with nanoliter volume resolution by NMR Cryoporometry", *Langmuir* **24**, 4470-4472.
- [17] Ambari, A., Benhamou, M., Roux, S. and Guyon, E., 1990, "Pore size distribution in a porous medium obtained by a non-Newtonian fluid flow characteristic", *C.R. Acad. Sci. Paris*, t. **311**, série II, 1291-1295.
- [18] Siddiqui, S. U., and Mishra, S., 2007, "A study of modified Casson's fluid in modelled normal and stenotic capillary-tissue diffusion phenomena", *J. Applied Mathematics and Computation* **189**, 1048–1057.